LIFEx v7.7.0

Announcement

— LIFEx —

C. Nioche, F. Orlhac, I. Buvat

What is new?

LIFEx version 7.7.0
Last update of document: 2024/10/01

LIFEx v7.7.0

Annoucement

— LIFEx —

Acknowledgements

Dear LIFEx users,

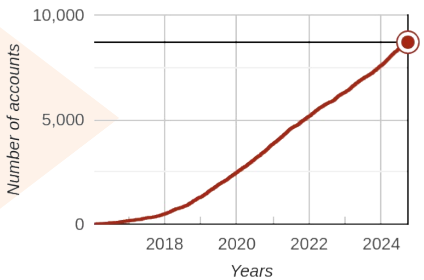

Evolution of the number of accounts (from our site web)

We are pleased to announce the release of LIFEx v7.7.0

We would like to take this opportunity to thank all 8.900 LIFEx users for their feedback and relevant suggestions. We took into account your comments to enhance the software and produce this version.
We hope you will enjoy it.

Do not hesitate to download this new release and replace your old LIFEx version. Your feedback will always be welcome.

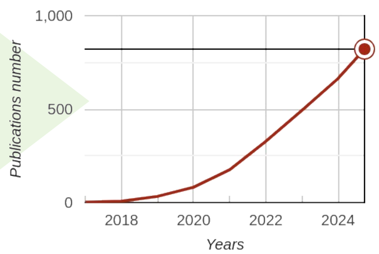

Evolution of Publications referencing LIFEx (from PubMed)

LIFEx is free of charge.

Please help us to keep it free by always quoting the LIFEx reference: (see below)

Please note that the correct reference to be cited is:
C Nioche, F Orlhac, S Boughdad, S Reuzé, J Goya-Outi, C Robert, C Pellot-Barakat, M Soussan, F Frouin, and I Buvat. LIFEx: a freeware for radiomic feature calculation in multimodality imaging to accelerate advances in the characterization of tumor heterogeneity. Cancer Research 2018; 78(16):4786-4789

LIFEx v7.7.0
Annoucement
— LIFEx —

Radiomics Theory And Practice
April 23-25, 2025, Paris

Dear LIFEx users,

For those who are interested, we organize a 3-day radiomics and LIFEx training session in April 2025 in Paris, France.

Space is limited to 20 participants on site as we will have a lot of hand-on sessions, so if you are willing to participate, please register early.

This year, we are opening the morning lectures to 50 virtual seats. Please let us know if you are interested (lectures +/- practical sessions). Practical sessions will be available for on-site attendees only.

This link to see preliminary programme.

This form to save your seat and register.

LIFEx v7.7.0

Annoucement

— LIFEx —

Interface screenshot

Christophe Nioche

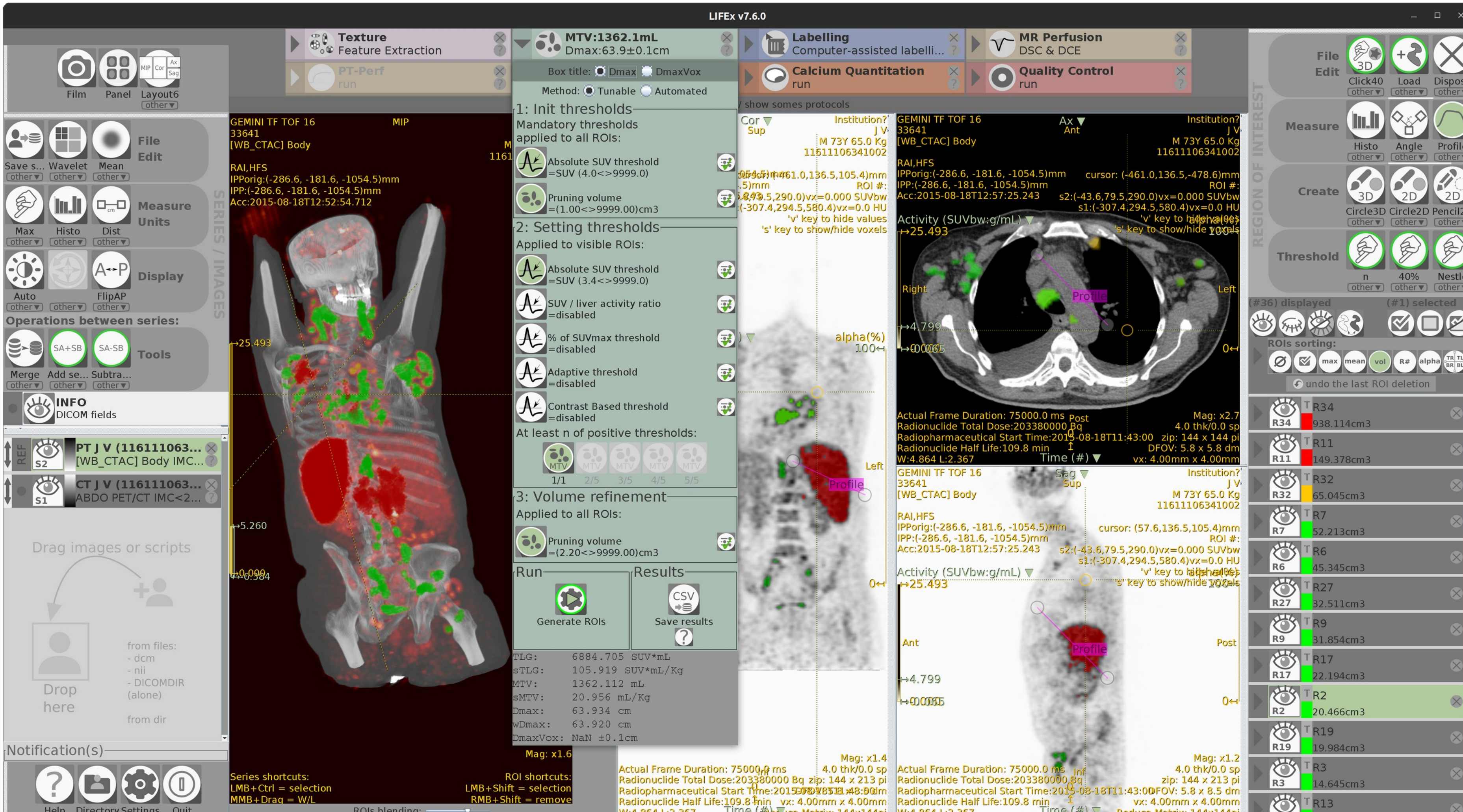

LIFEx v7.7.0

Annoucement

— LIFEx —

PET-CT Quality Control

Calibration and axial uniformity test

C. Nioche, M. Soret, C. Comtat

NEW

Main:

- This Quality Control (QC) protocol allows for the assessment of the quantification accuracy and the uniformity of a cylindrical phantom filled with an uniform activity concentration.
- It follows the guidelines of the PET working group of the French Society of Medical Physics (SFPM).

1.3.1 Calibration and axial uniformity test

A centered circular ROI is automatically drawn in yellow in each slice of the cylinder (see Figure 1.3).

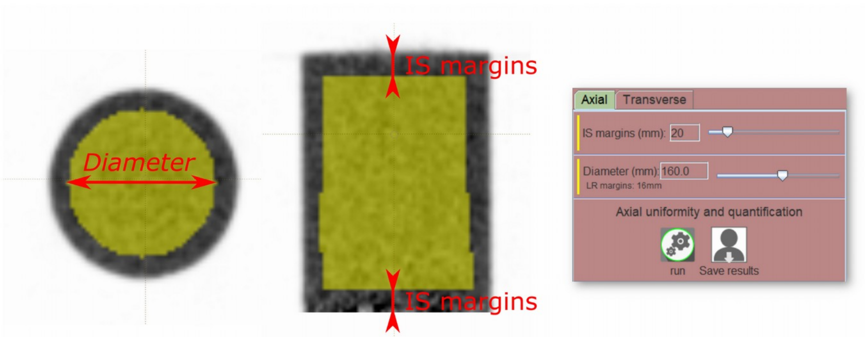

Figure 1.3: Definition of the ROIs for the calibration and axial uniformity test

The ROI mean value is automatically computed for each slice z: $ROI_{axial}(z)$. From these values, the following quantities are calculated with the *run* command (see Figure 1.4):

- the average: $\overline{ROI}_{axial} = Mean\{ROI_{axial}(z)\}$;
- the standard deviation: $\sigma(ROI_{axial}) = Standard\ deviation\{ROI_{axial}(z)\}$;
- the coefficient of variation: $c_V(ROI_{axial}) = \frac{\sigma(ROI_{axial})}{\overline{ROI}_{axial}}$;
- if the units are SUV body weight, the volumic bias: $\frac{\overline{ROI}_{axial}-1}{1}$;
- the minimum value: $min(ROI_{axial}) = Minimum\{ROI_{axial}(z)\}$;
- the maximum value: $max(ROI_{axial}) = Maximum\{ROI_{axial}(z)\}$;
- the axial integral uniformity: $IU_{axail} = \frac{max(ROI_{axial})-min(ROI_{axial})}{\overline{ROI}_{axial}}$.

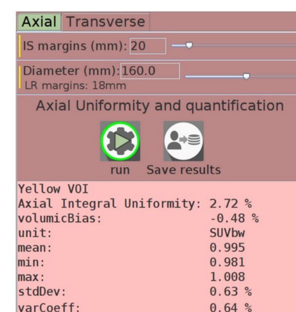

Figure 1.4: Results of the calibration and axial uniformity test

The results can be exported as a CSV ASCII file with the *Save_results* command.

LIFEx v7.7.0
Annoucement
— LIFEx —

PET-CT Quality Control
Calibration and Transverse uniformity test
C. Nioche, M. Soret, C. Comtat

NEW

Main:
- This Quality Control (QC) protocol allows for the assessment of the quantification accuracy and the uniformity of a cylindrical phantom filled with an uniform activity concentration.
- It follows the guidelines of the PET working group of the French Society of Medical Physics (SFPM).

1.3.2 Transverse uniformity test

A centered circular ROI in green and four peripheral circular ROIs in red are automatically drawn in each slice of the cylinder (see Figure 1.5).

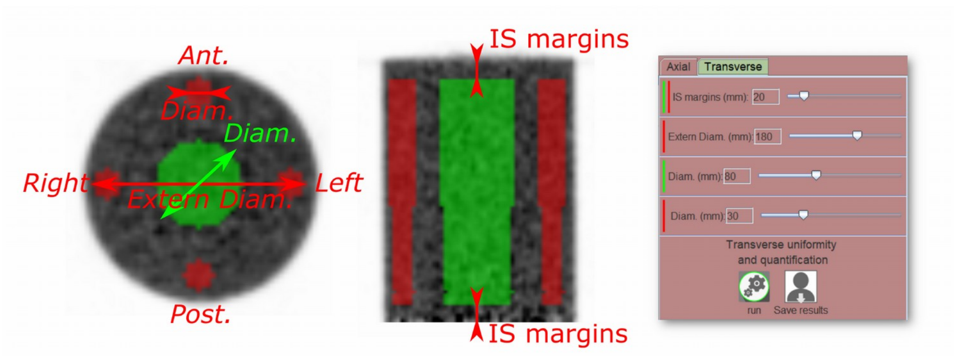

Figure 1.5: Definition of the ROIs for the transverse uniformity test

From these values, the transverse integral uniformity is automatically computed for each slice as:

$$IU_{transverse}(z) = \frac{max_{transverse}(z) - min_{transverse}(z)}{mean_{transverse}(z)} \quad (1.1)$$

- the average: $\overline{IU}_{transverse} = Mean\{IU_{transverse}(z)\}$;
- the central value: $IU_{transverse}(z_c)$ on the central slice z_c;
- the minimum value: $min(IU_{transverse}) = Minimum\{IU_{transverse}(z)\}$;
- the maximum value: $max(IU_{transverse}) = Maximum\{IU_{transverse}(z)\}$;
- the global value, estimated on the volumic ROIs.

The results can be exported as a CSV ASCII file with the *Save_results* command.

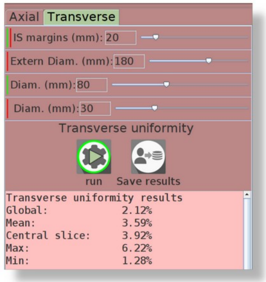

Figure 1.6: Results of the transverse uniformity test

LIFEx v7.7.0
Annoucement
— LIFEx —

PET-CT Quality Control
NEMA IEC PET Body Phantom Set

C. Nioche, M. Soret, C. Comtat

NEW

Main:
- This test allows for the evaluation of the PET system image quality in a standardized situation representative of a typical clinical condition. It is a global measure that includes data acquisition and image reconstruction and quantification steps.
- It follows the guidelines of the PET working group of the French Society of Medical Physics (SFPM).

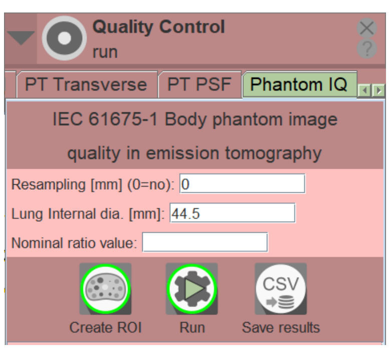

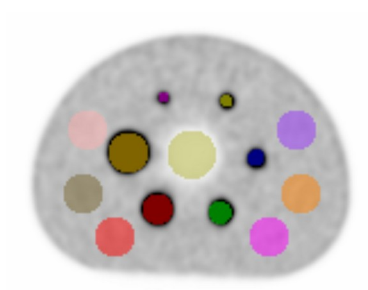

2.4.1 Body background

Six spherical VOIs with a diameter of 37 mm are automatically drawn in the background. The mean and standard-deviation of the activity concentration in each background VOI I are reported: BGSphere$I$_Mean and BGSphere$I$_Dev. The averaged activity concentration across the six VOIs is also reported: BGSpheres_Mean.

2.4.2 Contrast spheres

A spherical VOI is automatically drawn for each of the six contrast sphere, with a diameter equal to the nominal internal diameter D of the sphere. Its theoretical volume $\frac{4}{3}\pi\left(\frac{D}{2}\right)^3$ and effective volume, depending on the voxel sampling, are reported.

The mean and standard-deviation of the activity concentration in the contrast spheres VOI of diameter D are reported: Sphere$D$_Mean and Sphere$D$_Dev.

The measured activity concentration ratios between the contrast spheres D and the body background are reported: Sphere$D$_RatioWithBGSM $= \frac{\text{Sphere}D\text{\_Mean}}{\text{BGSpheres\_Mean}}$.

The Contrast Recovery Coefficient (CRC) of each sphere D is then calculated as follows:

$$\text{Sphere}D\text{\_CRC} = \frac{\text{Sphere}D\text{\_RatioWithBGSM} - 1}{\text{Sphere}D\text{\_NominalRatio} - 1}, \quad (2.2)$$

where Sphere$D$_NominalRatio is the nominal ratio value.

2.4.3 Lung insert

A spherical VOI is automatically drawn on the cylindrical lung insert, with a diameter equal to the internal diameter of the insert.

The mean and standard-deviation of the activity concentration in the contrast lung VOI are reported: LungInsert_Mean and LungInsert_Dev.

The lung error is calculated as:

$$\text{LungError} = \frac{\text{LungInsert\_Mean}}{\text{BGSpheres\_Mean}}. \quad (2.3)$$

LIFEx v7.7.0

Annoucement

— LIFEx —

PET-CT Quality Control

Point Spread Function – spatial resolution

C. Nioche, M. Soret, C. Comtat

NEW

Main:

- This Quality Control (QC) protocol allows for the measurement of the spatial resolution under the conditions of a clinical oncological examination, that is to say in an attenuating and scattering medium.

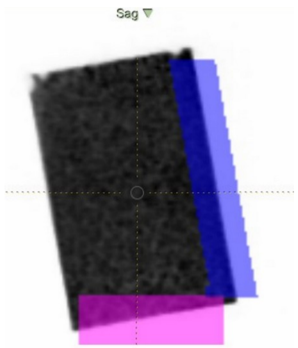

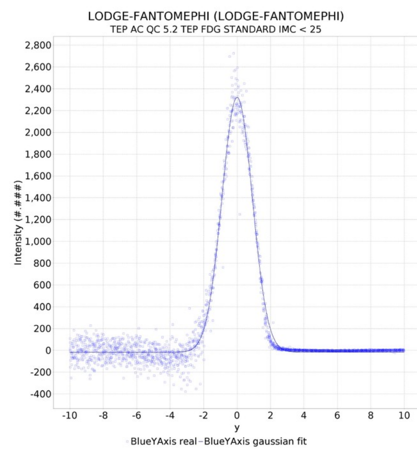

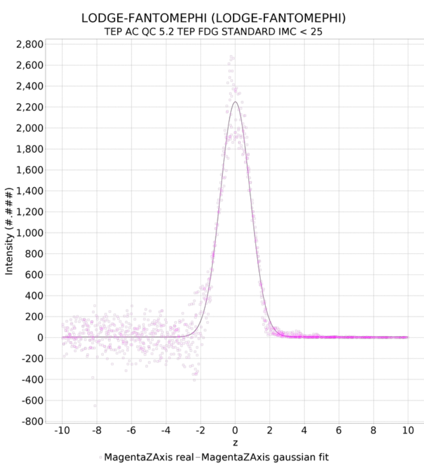

Figure 3.2: Spatial resolution in the axial direction. The blue dots indicate the data and the black curve indicate the Gaussian function fit from which the resolution measure is derived

- **Spatial Resolution in the Axial Direction:** An edge profile is drawn on the central axial slice, and on several slices in front and several slices behind (see Figure3.2). By appropriately displacing and then combining line profiles from different slices, the edge response function ESF(s) can be measured with a sampling interval much finer than the pixel spacing of the original images. From these composite-edge profiles ESF(s), the spatial resolution of the system can be determined by fitting an analytic function erf() and measuring the full width at half maximum (FWHM).

$$ESF(s) = \int_{-\infty}^{S} PSF(S')ds' \qquad (3.1)$$

$$PSF(s) = \frac{A}{\sigma\sqrt{2\pi}} e^{-(s-\mu)^2/2\sigma^2} \qquad (3.2)$$

$$ESF(s) = \frac{A}{2}\left(1 + erf\left(\frac{s-\mu}{\sigma\sqrt{2}}\right)\right) \qquad (3.3)$$

$$FWHM = \sqrt{8\ln 2}\sigma \qquad (3.4)$$

Where ESF(s) is the edge function, PSF(s) is the point spread function of the signal, A is a scaling factor which takes into account the magnitude of the data, μ is the center of the Gaussian function, and σ is the standard deviation of the Gaussian function.

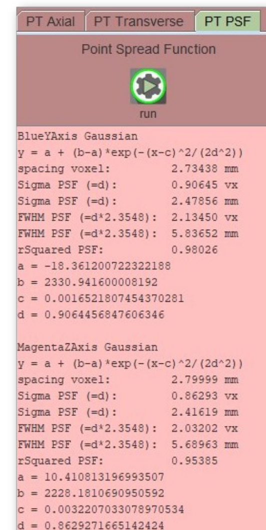

- **Spatial Resolution in the Radial Direction:** An edge profile is drawn on the central coronal slice and on several slices to the left and right. In a manner similar to the axial step, the spatial resolution is obtained.

LIFEx v7.7.0
Annoucement
— LIFEx —

New radiomic features
NHOC and NHOP definitions
Narinée Hovhannisyan-Baghdasarian

NEW

Narinée Hovhannisyan-Baghdasarian, Marie Luporsi, Nicolas Captier, Christophe Nioche, Vesna Cuplov, Erwin Woff, Nadia Hegarat, Alain Livartowski, Nicolas Girard, Irène Buvat, Fanny Orlhac. Promising candidate prognostic biomarkers in [18F]FDG-PET images: Evaluation in independent cohorts of Non–Small Cell Lung Cancer Patients. Journal of Nuclear Medicine March 2024, jnumed.123.266331; DOI: https://doi.org/10.2967/jnumed.123.266331

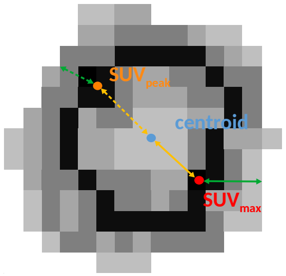

A Tumor
(black is high SUV, white is low SUV)

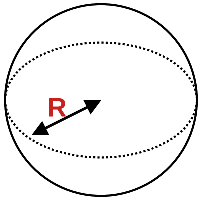

B Hypothetical sphere of radius R
having the same volume as the tumor

NHOCmax: distance (yellow arrow)
from the voxel with maximum SUV (SUVmax, red cercle)
to the tumor centroid (blue cercle) divided (normalized) by the radius (R)

NHOCpeak: normalized distance (yellow dashed arrow)
from the hotspot with maximum average SUV
(within a $1cm^3$ spherical volume, SUVpeak, orange cercle)
to the tumor centroid

NHOPmax: normalized distance (green line)
from the SUVmax
to the tumor perimeter (closest border)

NHOPpeak: normalized distance (green dashed line)
from the SUVpeak
to the tumor perimeter

LIFEx features in relation:

NHOCmax:	MORPHOLOGICAL_radiusSphereNorm_MaxIntensityCoor_RoiCentroidCoor_Dist
NHOCpeak:	MORPHOLOGICAL_radiusSphereNorm_PeakIntensityCoor_RoiCentroidCoor_Dist
NHOPmax:	MORPHOLOGICAL_radiusSphereNorm_MaxIntensityCoor_PerimeterCoor_3DSmallestDist
NHOPpeak:	MORPHOLOGICAL_radiusSphereNorm_PeakIntensityCoor_PerimeterCoor_3DSmallestDist

LIFEx v7.7.0

Annoucement

— LIFEx —

New radiomic features

Opened to the public

Narinée Hovhannisyan-Baghdasarian

NEW

*MORPHOLOGICAL_** Features:

maxIntensityCoor_RoiCentroidCoor_Dist
radiusSphereNorm_MaxIntensityCoor_RoiCentroidCoor_Dist **(NHOCmax)**
radiusRoiNorm_MaxIntensityCoor_RoiCentroidCoor_Dist
peakIntensityCoor_RoiCentroidCoor_Dist
radiusSphereNorm_PeakIntensityCoor_RoiCentroidCoor_Dist (**NHOCpeak**)
radiusRoiNorm_PeakIntensityCoor_RoiCentroidCoor_Dist
radiusSphereNorm_CentroidCoor_WcentroidCoor_Dist
radiusRoiNorm_CentroidCoor_WcentroidCoor_Dist
maxIntensityCoor_PerimeterCoor_3DSmallestDist
radiusSphereNorm_MaxIntensityCoor_PerimeterCoor_3DSmallestDist (**NHOPmax**)
radiusRoiNorm_MaxIntensityCoor_PerimeterCoor_3DSmallestDis
maxIntensityCoor_PerimeterCoor_2DAxialSmallestDist
radiusSphereNorm_MaxIntensityCoor_PerimeterCoor_2DAxialSmallestDist
radiusRoiNorm_MaxIntensityCoor_PerimeterCoor_2DAxialSmallestDist
maxIntensityCoor_PerimeterCoor_2DCoronalSmallestDist
radiusSphereNorm_MaxIntensityCoor_PerimeterCoor_2DCoronalSmallestDist
radiusRoiNorm_MaxIntensityCoor_PerimeterCoor_2DCoronalSmallestDist
maxIntensityCoor_PerimeterCoor_2DSagittalSmallestDist
radiusSphereNorm_MaxIntensityCoor_PerimeterCoor_2DSagittalSmallestDist
radiusRoiNorm_MaxIntensityCoor_PerimeterCoor_2DSagittalSmallestDist
peakIntensityCoor_PerimeterCoor_3DSmallestDist
radiusSphereNorm_PeakIntensityCoor_PerimeterCoor_3DSmallestDist (NHOPpeak)
radiusRoiNorm_PeakIntensityCoor_PerimeterCoor_3DSmallestDist
peakIntensityCoor_PerimeterCoor_2DAxialSmallestDist
radiusSphereNorm_PeakIntensityCoor_PerimeterCoor_2DAxialSmallestDist
radiusRoiNorm_PeakIntensityCoor_PerimeterCoor_2DAxialSmallestDist
peakIntensityCoor_PerimeterCoor_2DCoronalSmallestDist
radiusSphereNorm_PeakIntensityCoor_PerimeterCoor_2DCoronalSmallestDist
radiusRoiNorm_PeakIntensityCoor_PerimeterCoor_2DCoronalSmallestDist
peakIntensityCoor_PerimeterCoor_2DSagittalSmallestDist
radiusSphereNorm_PeakIntensityCoor_PerimeterCoor_2DSagittalSmallestDist
radiusRoiNorm_PeakIntensityCoor_PerimeterCoor_2DSagittalSmallestDist

LIFEx v7.7.0

Annoucement

— LIFEx —

New predictive model

PREDICTOR-HNC

Arnaud Beddok

NEW

Arnaud Beddok, Fanny Orlhac, Valentin Calugaru, Laurence Champion, Catherine Ala Eddine, Christophe Nioche, Gilles Créhange, Irène Buvat. [18F]-FDG PET and MRI radiomic signatures to predict the risk and the location of tumor recurrence after re-irradiation in head and neck cancer. Eur J Nucl Med Mol Imaging. 2023 Jan;50(2):559-571. doi: 10.1007/s00259-022-06000-7

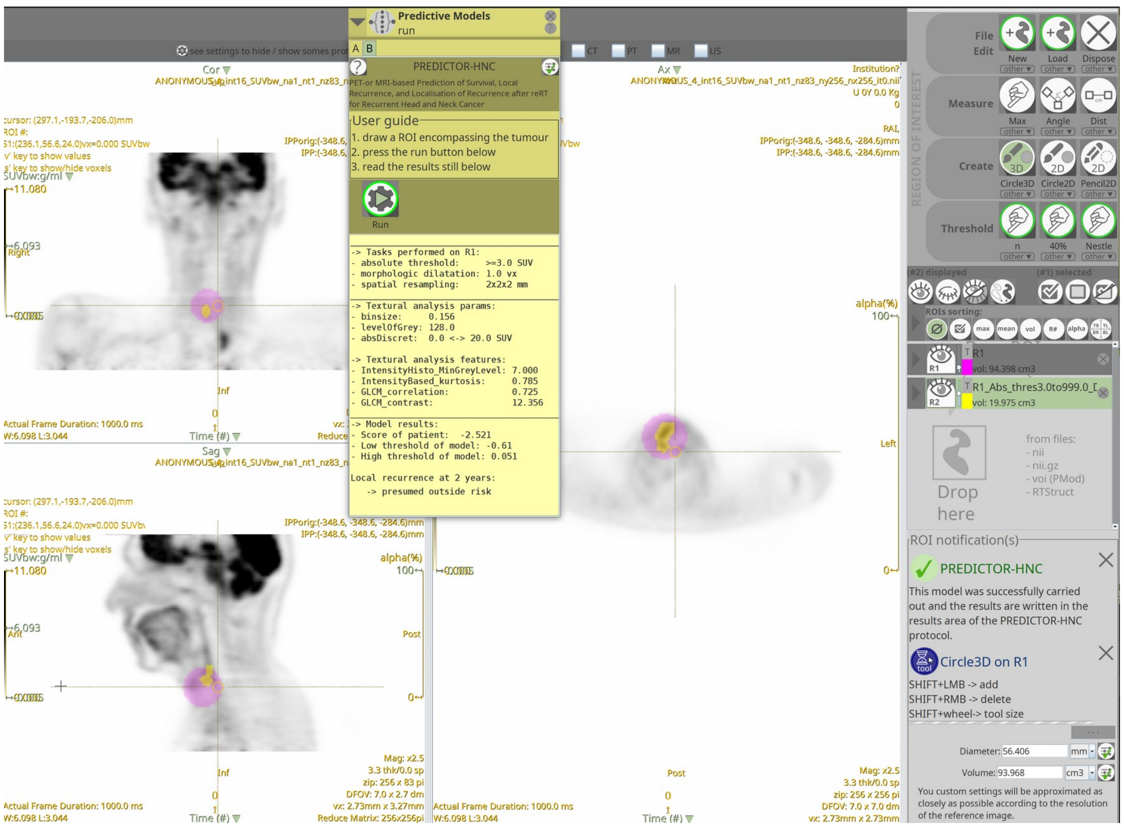

Purpose:

To evaluate whether radiomics from [18F]-FDG PET before re-irradiation (reRT) of recurrent head and neck cancer (HNC) could predict the occurrence and the location “in-field” or “outside” of a second loco-regional recurrence (LR).

LIFEx is still evolving

Christophe Nioche

Other functionalities are being added every week.
Stay tuned !
We hope you go on enjoying LIFEx !

Awards

2018 The Best of THE AACR JOURNALS — A COLLECTION OF THE MOST-CITED RESEARCH ARTICLES

2020 Prix unicancer de l'innovation — 6e édition

LIFEx is free of charge.

Please help us to keep it free by always quoting the LIFEx reference: (see below)

Please note that the correct reference to be cited is:
C Nioche, F Orlhac, S Boughdad, S Reuzé, J Goya-Outi, C Robert, C Pellot-Barakat, M Soussan, F Frouin, and I Buvat. **LIFEx: a freeware for radiomic feature calculation in multimodality imaging to accelerate advances in the characterization of tumor heterogeneity.** Cancer Research 2018; 78(16):4786-4789